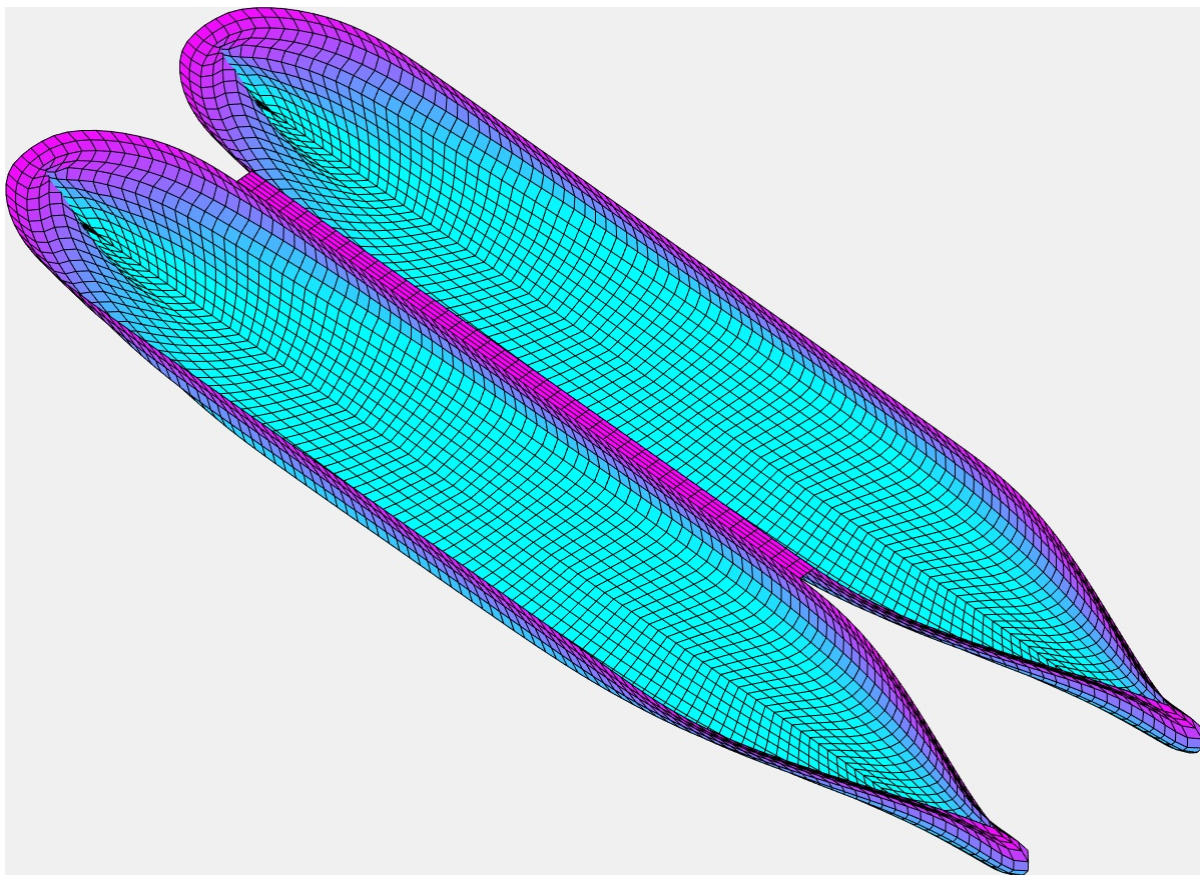


# Comparison of WAMIT v7.3 with Marin Model Tests for Side-by-Side LNG Carriers in Waves

Tim Gourlay

Perth Hydro Research Report R2019-08



Document History	
26 November 2019	Report published

## SUMMARY

This validation study uses model tests undertaken at Marin and described in Pauw et al. (2007), simulating side-by-side LNG carriers in head-sea waves. Model test results are compared with numerical predictions using WAMIT v7.3, with and without a damping lid.

## CONTENTS

1. Test case .....	3
2. WAMIT calculations with optional gap lid .....	5
3. Mesh dependency results with no gap lid.....	6
4. Results for fixed ship, wave load RAOs .....	7
5. Results for fixed ship, wave RAOs on gap centreline .....	8
6. Results for free ship, wave RAOs on gap centreline .....	9
7. Results for free ship, motion RAOs .....	10
8. Conclusions .....	11
9. Acknowledgements.....	11
10. References.....	11

## 1. Test case

The test case is described in Pauw et al. (2007) and Bunnik et al. (2009). It consists of a 1:50-scale LNG carrier close to a basin wall, representative of two identical side-by-side LNG carriers.

Particulars of the LNG carrier(s) and test setup are shown in Table 1.

Length between perpendiculars	274.0 m
Beam	44.2 m
Depth	25.0 m
Draught	11.0 m
Displacement	97759 tonnes
Block coefficient	0.716
Vertical Centre of Gravity	16.1 m above keel
Longitudinal Centre of Gravity	-1.1 m forward of Station 10
Transverse Metacentric Height (GM)	5.0 m
Roll Radius of Gyration	16.3 m
Pitch Radius of Gyration	70.1 m
Yaw Radius of Gyration	70.0 m
Water Depth	37.5 m
Gap to Basin Wall	2.0 m
Gap to Image LNGC	4.0 m

**Table 1: Particulars of the LNG carrier test setup. All dimensions given at full scale.**

Surface meshes for the LNG carrier up to the waterline, at various refinements, were provided by Marin for this study. The three surface meshes used in this study are shown in Figure 1.

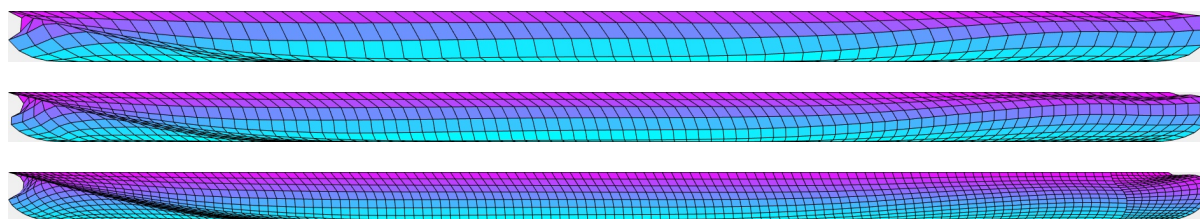


**Figure 1: LNG carrier surface meshes provided by Marin, without hull lids. (Top) 1040-panel mesh; (Middle) 2376-panel mesh; (Bottom) 5296-panel mesh.**

For the side-by-side case, both vessels need to be meshed, together with an optional gap lid in between them. An example combined mesh is shown in Figure 2.

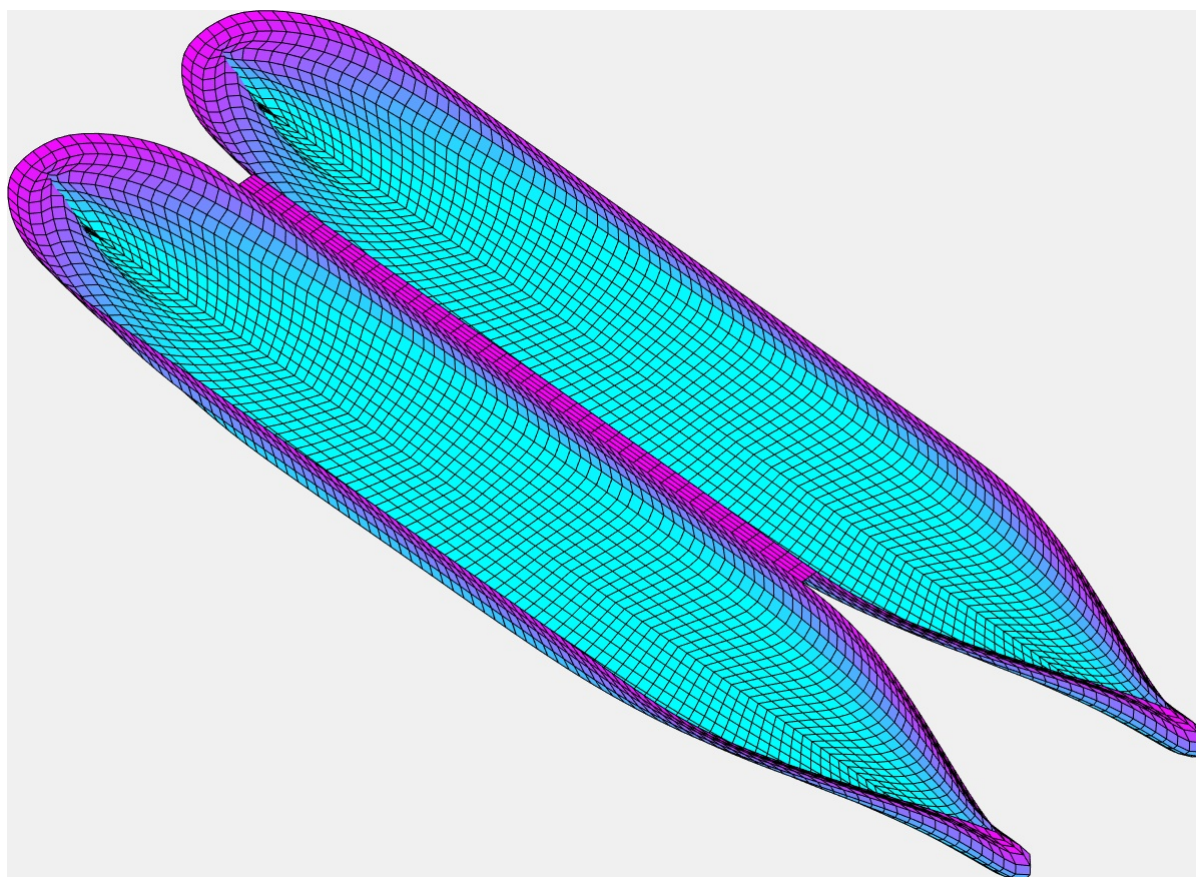


Figure 2: Perspective view of 2376-panel meshes of side-by-side LNG carriers, together with 160-panel gap lid on free surface between hulls; total 4912 panels

## 2. WAMIT calculations with optional gap lid

The use of a lid between side-by-side vessels is a popular technique for damping wave elevations in the gap, dating back to Huijsmans et al. (2001), Newman (2003) and Chen (2005). The 2019 version of WAMIT (version 7.3) allows for the inclusion of a damping gap lid without the need for generalized modes.

For panels on the gap lid, the free-surface boundary condition (WAMIT 2019, eq. 15.92) is

$$\omega^2 \phi - g \phi_z = i \omega \varepsilon_{WAMIT} \phi_z \quad \text{on } z = 0 \quad (1)$$

where the total potential (WAMIT 2019, eq. 2) is

$$\Phi = \text{Re}\{\phi e^{i\omega t}\} \quad (2)$$

Here  $\omega$  is the wave circular frequency and  $g$  is the acceleration due to gravity.

According to Chen (2005, eq. 13) and Pauw et al. (2007), the damping lid equation used in HydroSTAR (H\*) is

$$\phi_z - (1 - i\varepsilon_{H*}) \frac{\omega^2}{g} \phi_z = 0 \quad \text{on } z = 0 \quad (3)$$

where the total potential (Chen 2005, eq. 3) is

$$\Phi = \text{Re}\{\varphi e^{-i\omega t}\} \quad (4)$$

Assuming epsilon is small, we can equate equations (1,2) with equations (3,4) to give

$$\varepsilon_{WAMIT} = \frac{g}{\omega} \varepsilon_{H*} \quad (5)$$

Therefore the “epsilon” value has different meaning in WAMIT to its meaning in HydroSTAR. For these calculations we have used  $\varepsilon_{WAMIT} = 0.2$  across all wave frequencies.

Other WAMIT settings used in this study are described in Table 2.

WAMIT solver	Direct solver, source method
Degrees of freedom	Coupled 6-DoF
First-order wave loads method	Diffraction potential
Second-order wave loads method	Pressure integration
Irregular frequency removal	No
Separate integration of logarithmic singularity	No
Viscous roll damping	No
Gap lid method	Free, impervious

Table 2: WAMIT solver settings used in the study

Only head seas were used in the model tests and calculations.

### 3. Mesh dependency results with no gap lid

Mesh dependency is studied with reference to the wave load response amplitude operators (RAOs). Results are shown in Figure 3.

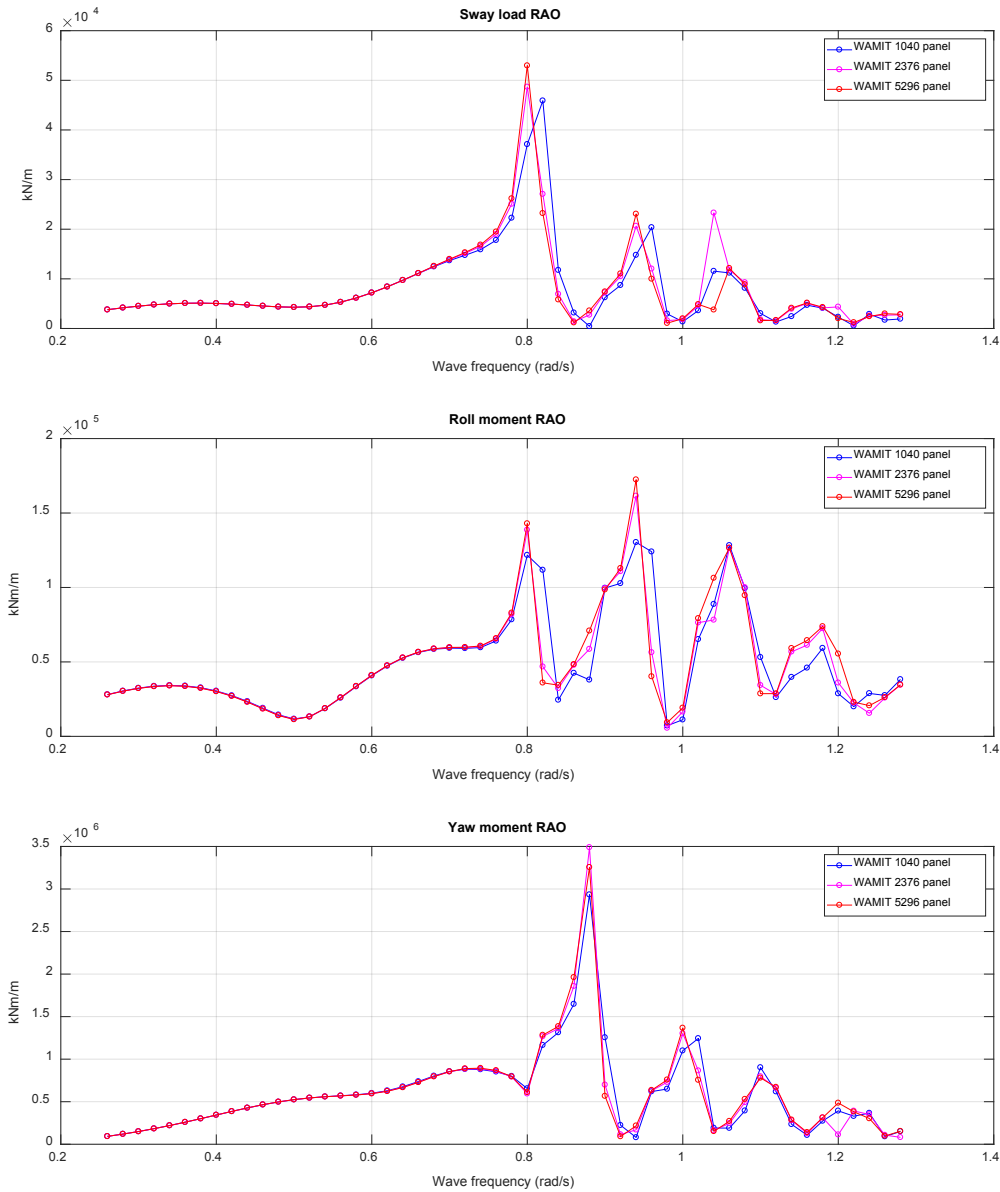


Figure 3: Mesh dependency study using wave load RAOs and no gap lid

We see that results are indistinguishable at frequencies up to 0.7 rad/s (wave periods above 9 seconds). At higher frequencies, the 1040-panel mesh may be too coarse. Overall, the 2376-panel mesh offers a good compromise between mesh convergence and computational efficiency. The 2376-panel hull mesh was used for all subsequent calculations in this report.

### 4. Results for fixed ship, wave load RAOs

Wave loads were measured using a white noise spectrum, with the model fixed (Pauw et al. 2007, Fig. 6). Results for the asymmetric model (sway and yaw) are shown in Figure 4, together with WAMIT results with or without a damping lid between the hulls. Roll moment results are not shown, as these are measured about the centre of gravity in the model tests, but about the waterline in the WAMIT results. Roll angle comparisons are given in Section 7.

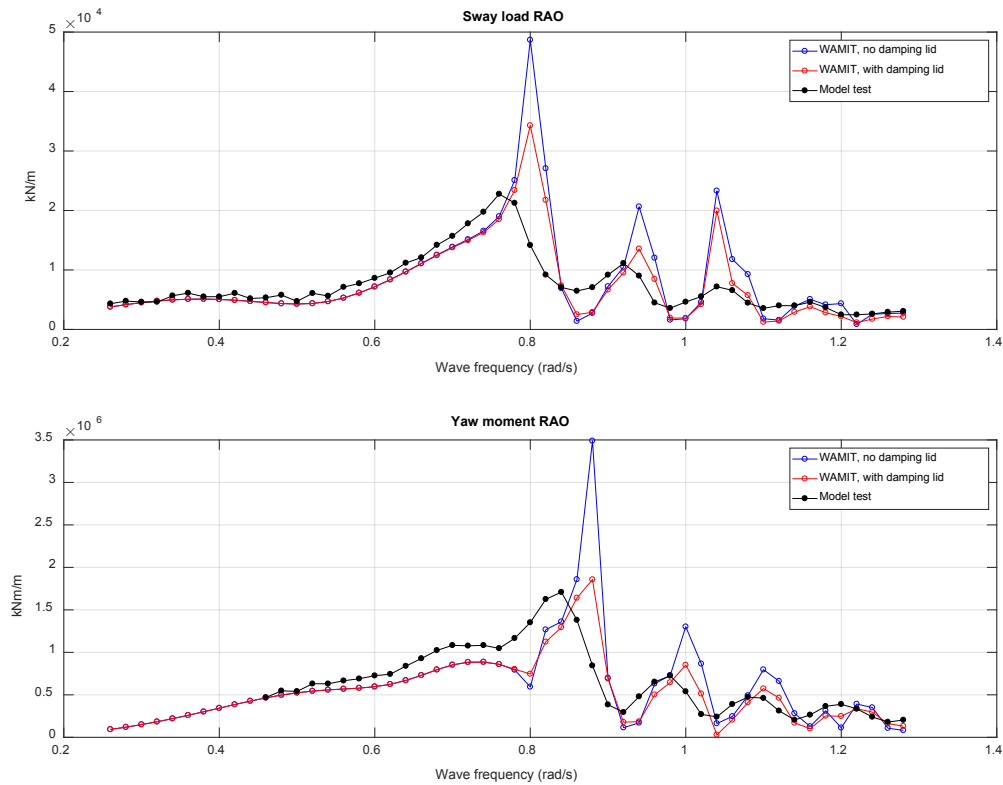


Figure 4: Wave load RAO comparisons between WAMIT and model tests. Model test results from Pauw et al. (2007, Fig. 6).

### 5. Results for fixed ship, wave RAOs on gap centreline

The head-sea model tests included measurements of diffracted wave amplitude on the basin wall, corresponding to the centreline between side-by-side ships. Results are shown in Figure 5, together with WAMIT predictions.

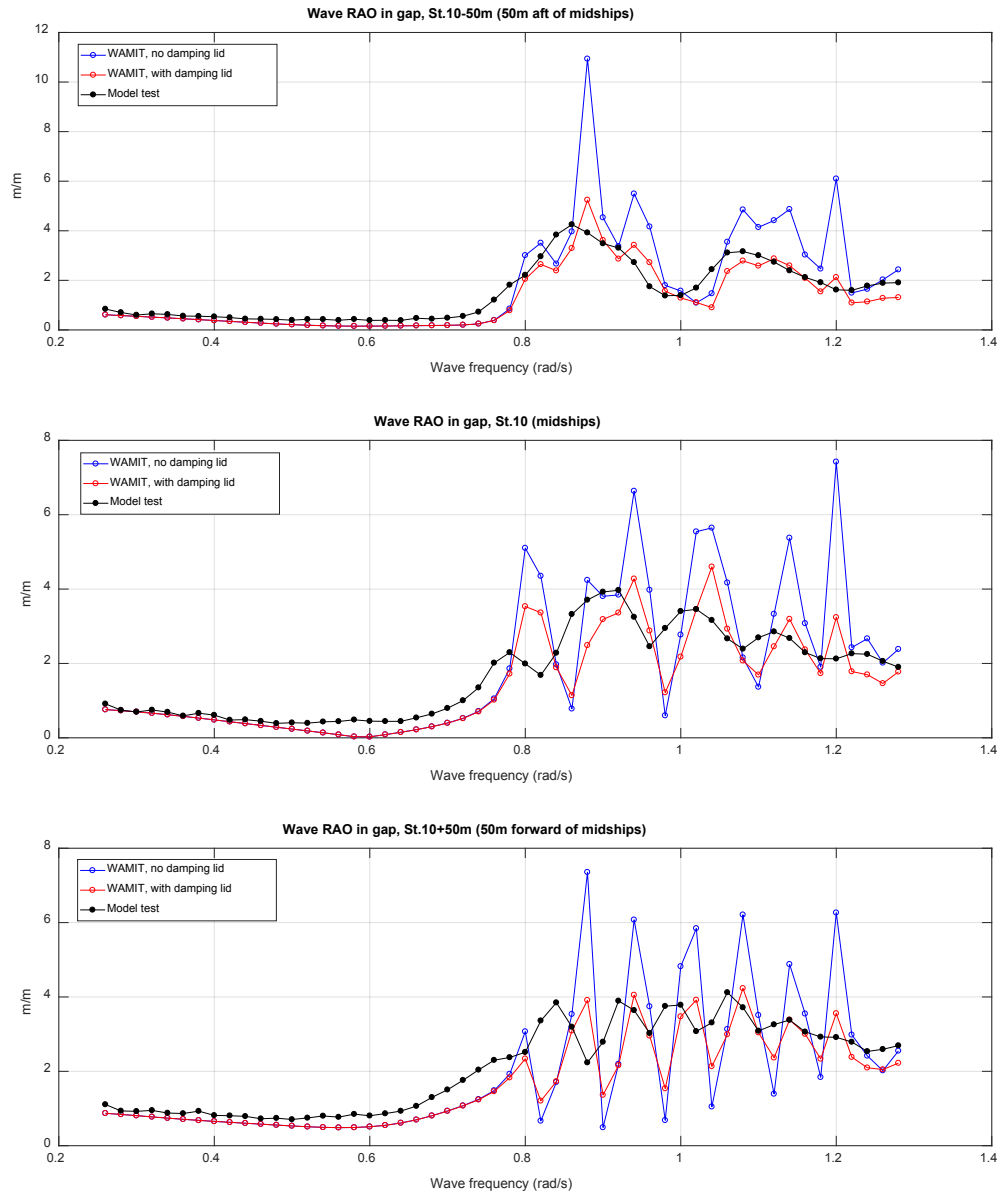


Figure 5: Wave RAO comparisons between WAMIT and model tests, for the fixed-ship case. Model test results from Pauw et al. (2007, Fig. 8).

### 6. Results for free ship, wave RAOs on gap centreline

Wave amplitudes on the gap centreline were measured with the model free to oscillate in a soft mooring arrangement (Pauw et al. 2007, Fig. 9). In this case, operational sea states with peak periods from 5 – 20 seconds were used in the model tests. Results are shown in Figure 6, together with WAMIT results.

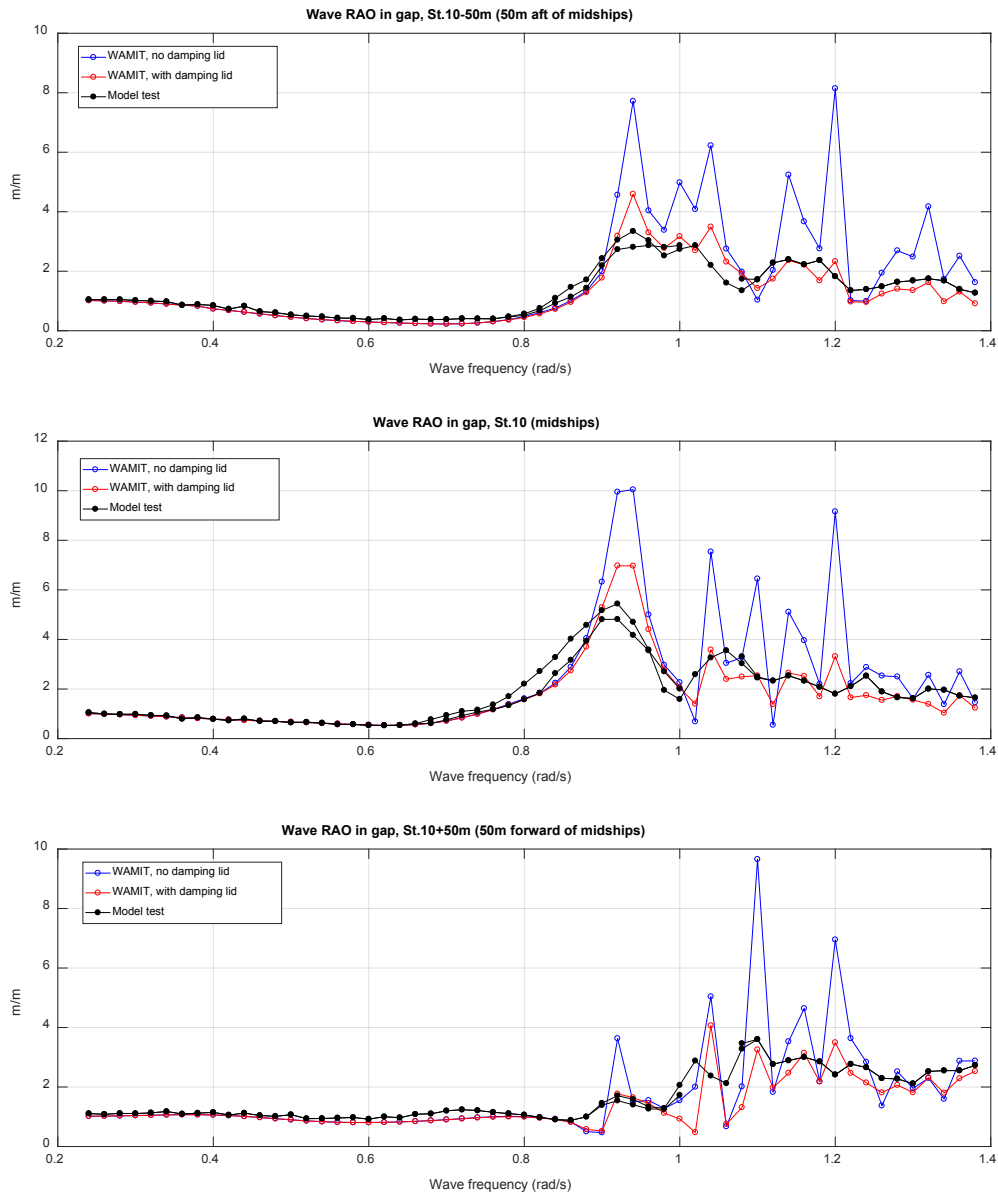


Figure 6: Wave RAO comparisons between WAMIT and model tests, for the free-ship case. Model test results from Pauw et al. (2007, Fig. 9).

## 7. Results for free ship, motion RAOs

Motion RAOs with a soft mooring arrangement were measured in the model tests. Results for the asymmetric modes (sway, roll and yaw) are shown in Figure 7, together with WAMIT results.

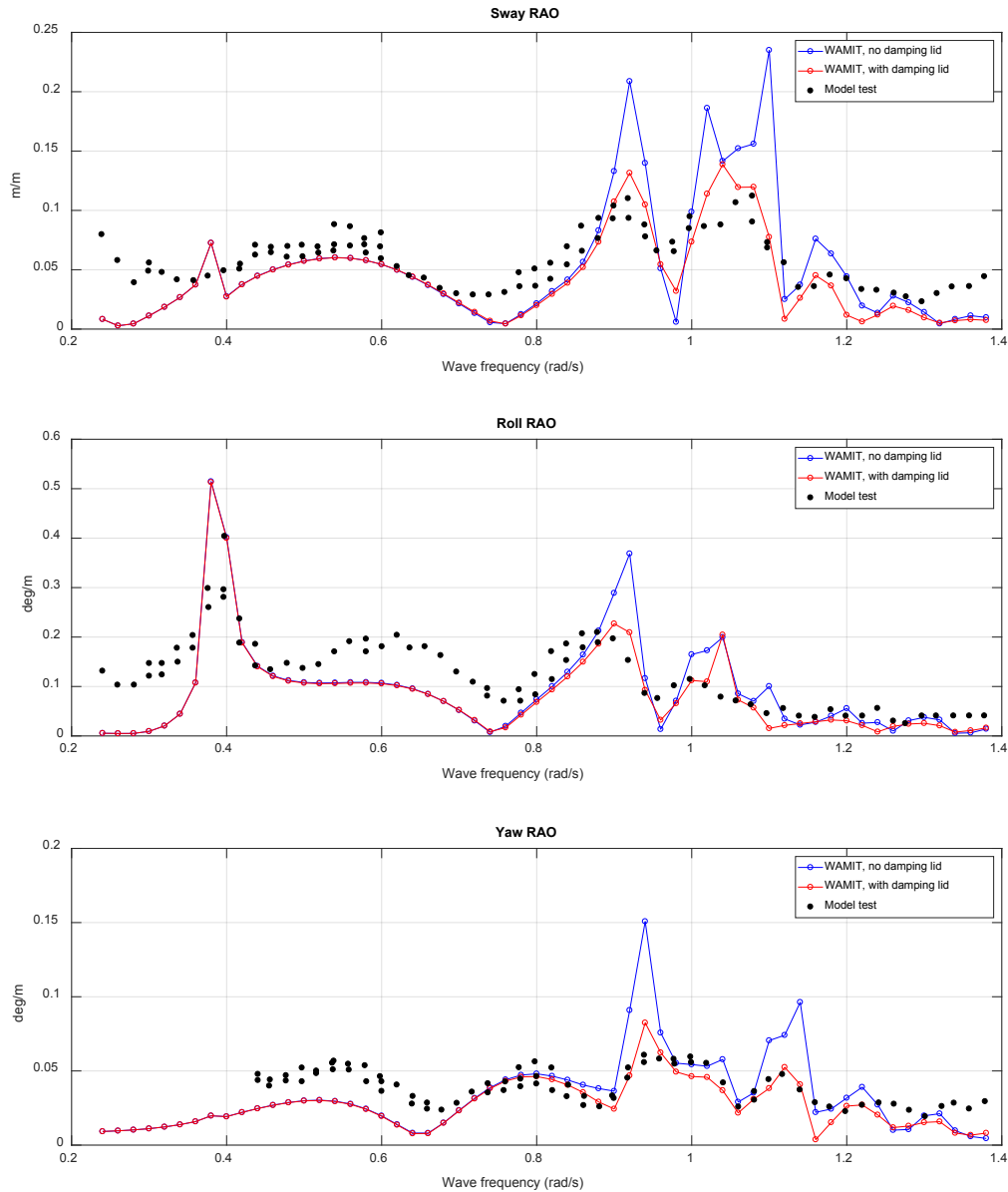


Figure 7: Motion RAO comparisons between WAMIT and model tests. Model test results from Pauw et al. (2007, Fig. 10).

## 8. Conclusions

Conclusions from the study were:

- The medium-refinement mesh (2376 panels) showed well-converged wave load results across all frequencies and allowed fast computation times.
- The inclusion of a damping lid in WAMIT makes negligible difference to wave loads, gap waves and motion RAOs at wave frequencies of up to 0.78 rad/s in this study (wave periods 8 seconds and above).
- The inclusion of a damping lid in WAMIT has a noticeable smoothing effect on wave loads, gap waves and motion RAOs at wave frequencies of 0.8 rad/s and above in this study, and brings the predictions closer to the model test results.
- First-order sway loads and yaw moments were quite well-predicted by WAMIT across all wave frequencies, with a slight shift in the peak frequency.
- For the ship vertically fixed, or free to oscillate, wave heights in the gap were quite well-predicted by WAMIT.
- Motion RAOs in sway, roll and yaw were quite well-predicted by WAMIT across all wave frequencies.

## 9. Acknowledgements

Information on the model tests was kindly provided by Willemijn Pauw and Tim Bunnik, of Marin, for this study. Surface meshes for the model-tested LNG carrier were kindly provided by Frédéric Jaouën, of Marin, for this study. The author acknowledges valuable discussions on the topic with Marin staff during recent research visits.

## 10. References

- Bunnik, T., Pauw, W.H., Voogt, A. 2009 Hydrodynamic analysis for side-by-side offloading. Proceedings of the 19th International Offshore and Polar Engineering Conference (ISOPE 2009), Osaka, Japan.
- Chen, X.-B. 2005 Hydrodynamic analysis for offshore LNG terminals. Proceedings of the 2nd International Workshop on Applied Offshore Mechanics, Rio de Janeiro, Brazil.
- Gourlay, T.P. 2019 A coupled ship and harbour model for dynamic mooring analysis in Geraldton Harbour. Proceedings, Coasts and Ports 2019, Hobart.
- Huijsmans, R.H.M., Pinkster, J.A., de Wilde, J.J. 2001 Diffraction and radiation of waves around side-by-side moored vessels. Proceedings of the 11th International Offshore and Polar Engineering Conference (ISOPE 2001), Stavanger, Norway.
- Newman, J.N. 2003 Application of generalized modes for the simulation of free surface patches in multiple body interactions. Proceedings of the 4th Annual WAMIT Consortium Meeting, Woods Hole, USA.
- Pauw, W.H., Huijsmans, R.H.M., Voogt, A. 2007 Advances in the hydrodynamics of side-by-side moored vessels. Proceedings of the 26th International Conference on Offshore Mechanics and Arctic Engineering (OMAE 2007), San Diego, USA.
- WAMIT 2019 WAMIT v7.3 User Manual, WAMIT Inc.